Catal Lett (2008) 120:148–153
DOI 10.1007/s10562-007-9267-6

Study on the Reaction Mechanism for Soot Oxidation Over TiO_2 or ZrO_2-supported Vanadium Oxide Catalysts by Means of In-situ UV-Raman

Jian Liu · Zhen Zhao · Peng Liang · Chunming Xu · Aijun Duan · Guiyuan Jiang · Wenyong Lin · Israel E. Wachs

Received: 30 August 2007 / Accepted: 3 September 2007 / Published online: 19 September 2007

Abstract The reaction mechanisms for diesel soot oxidation over V_4/ZrO_2 or V_4/TiO_2 oxide catalysts were studied by the means of in-situ UV-Raman spectroscopy. The results indicate that the formation of surface oxygen complexes (SOC) is a key step and the SOC species mainly exist as carboxyl groups. The presence of NO in the reaction gas stream can promote the formation of SOC species. For soot oxidation over V_4/TiO_2 catalyst, NO_2 can be produced and remarkably accelerate soot oxidation. Based on the UV-Raman experimental results, two different reaction mechanisms are proposed for soot oxidation over V_4/ZrO_2 or V_4/TiO_2 samples, respectively.

Keywords Supported vanadium oxide · Catalyst · UV-Raman · In-situ · Soot · Reaction mechanism

1 Introduction

Soot particulate (PM) emitted from diesel engines is a serious contamination in urban areas. The combination of traps and oxidation catalysts appears to be one of the most efficient after-treatment techniques. The role of the catalyst here is to reduce soot ignition temperature and enhance the oxidation rate of the soot collected on the filter during trap regeneration [1]. A great deal of attention has been given in the last 20 years to the research of soot catalytic combustion. Recently, some researches reported that vanadium-based catalysts were one of the most promising systems for the oxidation of diesel soot [1–3]. However, several problems are still unsolved, although the amount of work towards a better understanding is impressive. In particular, the reaction mechanism of the catalytic oxidation of soot remains unclear. It is due to the deep black colour of soot, which causes that it is very difficult in acquiring some useful information about the catalytic oxidation of soot under real reaction conditions. Some researchers investigated the catalytic oxidation of carbonaceous materials by means of in-situ IR spectroscopy using KBr as diluent [4, 5]. While the interactions between soot, metal oxides, and KBr cannot be excluded, especially when analysis is performed at high temperature. In this paper, the in-situ UV-Raman was first employed to investigate the mechanism of soot oxidation over supported vanadia catalysts. It was verified that the formation of SOC, which mainly existed as carboxyl groups, was the main reaction process during the soot oxidation over V_4/ZrO_2 or V_4/TiO_2 catalyst.

On the other hand, Oi-Uchisawa et al. [6, 7] reported that Pt catalysts exhibited a high level of catalytic activity to promote soot oxidation in recent years. Platinum is supposed to oxidize NO to NO_2, which subsequently oxidizes soot to CO and CO_2. Therefore, NO_2 is used as an intermediate to facilitate an indirect contact between the platinum catalyst and soot. The high oxidation rate of soot is due to the strong oxidizing ability of NO_2. This catalyst system is the best one so far reported for soot oxidation under loose contact conditions. However, Pt is very

J. Liu · Z. Zhao (✉) · C. Xu · A. Duan · G. Jiang
State Key Laboratory of Heavy Oil Processing, China University of Petroleum, Beijing 102249, China
e-mail: zhenzhao@cup.edu.cn

P. Liang
Material Science & Chemical Engineering School, Eastern Liaoning University, Dandong, Liaoning 118003, China

W. Lin · I. E. Wachs
In-situ Molecular Characterization and Catalysis Laboratory, Department of Chemical Engineering, Lehigh University, Bethlehem, PA 18015, USA

expensive. Thus, it will be an optimal method if NO_2 can be produced and catalyze soot oxidation on the non-noble metal catalysts. In the present study a similar mechanism, i.e., the direct evidence for NO_2 indirectly catalytic function is found by the means of UV-Raman spectroscopic detection on the V_4/TiO_2 catalyst. Due to its strong oxidizing ability, the soot oxidation can be remarkably accelerated by NO_2. Therefore, V_4/TiO_2 catalyst has higher activity than V_4/ZrO_2 catalyst for soot oxidation.

2 Experimental

Printex-U, which was supplied by Degussa, was used as model soot. The two samples of supported vanadia catalysts were named as V_4/ZrO_2 or V_4/TiO_2, respectively, where the subscript 4 stands for the number of V atoms per 100 support metal ions. The preparation and activity measurement methods of the catalysts were described in detail in our previous work [1].

Vis-Raman spectra were performed on LabRam HR spectrometer manufactured by Horiba Jobin Yvon Company, France. The laser excitation wavelength was 514 nm. UV-Raman spectra were collected at a Jobin Yvon LabRam-HR equipped with a confocal microscope, 2,400/900 grooves/mm gratings and a notch filter. The laser excitation at 325 nm was generated from a He–Cd laser. The spectrometer resolution was less than 2 cm^{-1}. The in-situ UV-Raman studies of soot oxidation over supported vanadia catalysts were loaded in powder form into an in-situ cell (Linkam, TS1500). The quartz cell is capable of operating up to 650 °C. The catalyst and soot (10:1, w/w) were carefully mixed in an agate mortar in order to reproduce the tight contact mode. The in-situ UV-Raman spectra were collected at different temperatures after being dehydrated at 400 °C for 1 h in the flowing O_2/He to desorb the adsorbed moisture. During in-situ UV-Raman testing the reactant gas stream was passed through a mixture of the catalyst and soot at a flow rate of 50 mL/min using different gas compositions: (1) 5% O_2 and 0.2% NO balanced with He, or (2) 10% O_2 balanced with He.

3 Results and Discussion

Figure 1 shows the typical UV-Raman and Vis-Raman spectra of Printex U. For UV-Raman spectrum, a strong sharp peak appears at 1,585 cm^{-1} and a shoulder peak exists at 1,365 cm^{-1}. For Vis-Raman spectrum, two sharp peaks appear at 1,585 and 1,350 cm^{-1}, and their vibration intensities are basically same. According to the literature [8], the spectrum of soot generally exhibit two broad and strong overlapping peaks with intensity maxima at

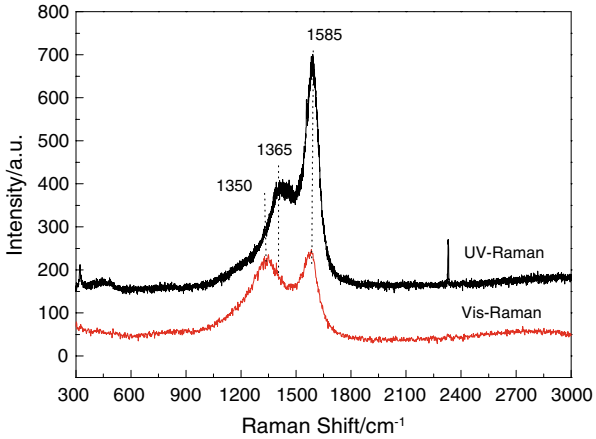

Fig. 1 The UV-Raman and Vis-Raman spectra of Printex U

$\sim$1,580 cm^{-1} and at $\sim$1,350 cm^{-1}. The band at around 1,580 cm^{-1} is corresponding to an ideal graphitic lattice vibration mode with E_{2g} symmetry, and the band at 1,350–1,365 cm^{-1} is assigned to a disorder graphitic lattice vibration mode with A_{1g} symmetry [8]. Compared to the Vis-Raman spectrum, the higher vibration intensity of the peak at 1,585 cm^{-1} in the UV-Raman spectrum indicates that UV-Raman is more sensitive to the E_{2g} symmetry vibration.

The investigation of the reaction mechanism of soot oxidation was carried out on V_4/ZrO_2 or V_4/TiO_2 catalysts. Figure 2 shows the in-situ UV-Raman spectra of V_4/ZrO_2 catalyst for soot oxidation at different temperatures. At (NO+O_2)/He atmosphere, as shown in Fig. 2a, the peaks below 1,200 cm^{-1} are due to the vanadyl or zirconium oxides. The peak at 1,584 cm^{-1} is corresponding to an ideal graphitic lattice vibration mode with E_{2g} symmetry and at 1,365 cm^{-1} is assigned to the A_{1g} symmetry vibration of the disorder graphitic lattice. When reaction temperature exceeds 100 °C, two new peaks at 1,545 and 1,618 cm^{-1} appear in the UV-Raman spectra. According to the literature, the band at 1,545 cm^{-1} is ascribed to the ring stretching vibrations of aromatic moieties, and the band at 1,618 cm^{-1} may be assigned to the ν_A vibration of COO^- and benzene ring stretching. It indicates that the SOC species mainly exist as carboxyl groups [9]. With the increase of the reaction temperature, the intensities of the peaks gradually increase, indicating that the vibration enhances. When reaction temperature exceeds 300 °C, the intensities of the both peaks gradually decrease and they disappear at last. It may be due to the reaction has completed and soot has been completely oxidized. For soot oxidation over V_4/ZrO_2 catalyst at O_2/He atmosphere, as shown in Fig. 2b, the positions of the absorption peaks are basically unchanged compared with the UV-Raman spectra in Fig. 2a. It indicates that the peaks at 1,545 and

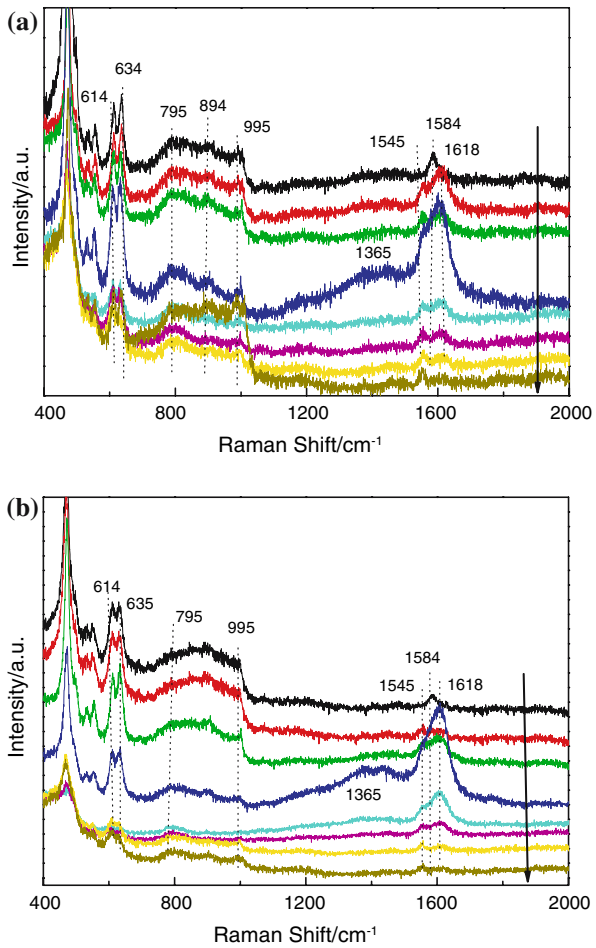

Fig. 2 The in-situ UV-Raman spectra of V_4/ZrO_2 catalyst during soot oxidation at different temperatures (lowest temperatures on top: ambient, 100, 200, 300, 400, 500, 600, and 650 °C). Reactant gas compositions: (**a**) 5% O_2 and 0.2% NO balanced with He and (**b**) 10% O_2 balanced with He

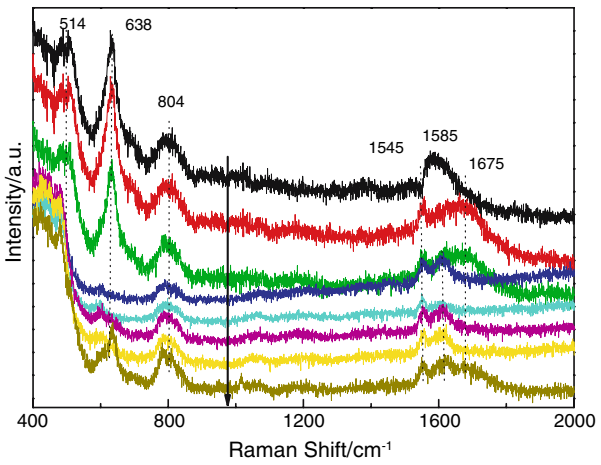

Fig. 3 The in-situ UV-Raman spectra of V_4/TiO_2 catalyst during soot oxidation at different temperatures (lowest temperatures on top: ambient, 100, 200, 300, 400, 500, 600, and 650 °C). Reactant gas compositions: 5% O_2 and 0.2% NO balanced with He

1,618 cm^{-1} cannot be attributed to the stretching vibration of the species containing nitrogen. Figure 2a shows that the peaks at 1,545 and 1,618 cm^{-1} appear in the UV-Raman spectra of V_4/ZrO_2 catalyst for soot oxidation at 100 °C. However, Fig. 2b shows that they do not appear until the reaction temperature reaches 200 °C. It indicates that the formation of SOC is easier in (NO + O_2)/He atmosphere than in O_2/He atmosphere.

Figure 3 shows the in-situ UV-Raman spectra of V_4/TiO_2 catalyst for soot oxidation at different temperatures. The reactant gases contains 5% O_2, 0.2% NO and diluted gas He. The peaks below 1,200 cm^{-1} are due to the vibration of vanadyl species or anatase. The peak at 1,585 cm^{-1} is assigned to the E_{2g} symmetry of soot. Several new vibration peaks at 1,545, 1,618 and 1,675 cm^{-1} appear in the UV-Raman spectra. The foregoing two peaks may be attributed to the vibration of carboxyl groups [9], and the last one may be due to the ν_{as} vibration of NO_2 [10, 11]. With the increase of the reaction temperature, the intensity of the peak at 1,675 cm^{-1} gradually decreases, and when the reaction temperature increases to 300 °C, the peak disappears. This phenomenon indicates that NO_2 has decomposed due to the thermodynamic unstablility of NO_2 at high temperature. However, a small amount of NO_2 is over again produced at 650 °C. It is ascribed to the complete oxidation of soot disturbing the chemical equilibrium of NO and NO_2. Thus, a very weak peak at 1,675 cm^{-1} appears again the UV-Raman spectra of V_4/TiO_2 catalyst.

The study on the mechanism for catalytic oxidation reactions of carbonaceous materials has been the subject of some researches over the last decades [12, 13]. In the previous studies, usually KBr was used as a diluent in IR spectroscopic studies to obtain high quality in-situ spectra of carbonaceous materials. However, interactions between SOC and/or metal oxides and KBr could not be excluded, especially when analyses were performed at elevated temperatures. While carbon black significantly absorbed IR radiation over the entire region from 400 to 4,000 cm^{-1}, therefore, it was limited to characterize the soot oxidation over metal oxides by using in-situ IR method. The Ultraviolet Raman spectroscopy is a powerful tool for the study of solid catalysts [14, 15]. UV-Raman can effectively monitor the reaction of soot oxidation over transition metal oxide catalysts. It does not need to dilute with KBr. In this study in-situ UV-Raman spectroscopy for the soot oxidation reaction was performed at various temperatures on the V_4/ZrO_2 and V_4/TiO_2 catalysts. Raman spectra taken during the oxidation of soot clearly show that the surface oxygen species can undergo significant structural changes depending on the oxidation temperature and the composition of the support. On V_4/TiO_2, the vibration band centered around 1,675 cm^{-1} may be assigned to the ν_{as}

vibration of NO_2 [10, 11]. Attributing to its thermodynamic unstablility, NO_2 will decompose with the increase of the reaction temperature. The in-situ UV-Raman spectra of V_4/TiO_2 exhibit that the intensity of the peak at 1,675 cm^{-1} gradually decreases and the peak disappears when the reaction temperature increases to 300 °C. On V_4/TiO_2 and V_4/ZrO_2, the peaks at 1,554 and 1,608 cm^{-1} indicate the formation of SOC on Printex-U in the presence of catalyst. It is different from the literature report that the SOC species mainly exist as quinine, lactones and ether-like complexes, and they are mainly present as carboxyl groups identified with in-situ UV-Raman spectroscopy in this work [13, 16]. Compared Fig. 2a with Fig. 3, it can be found that SOC appears on V_4/ZrO_2 at 100 °C, while it forms on V_4/TiO_2 at ambient temperature. It indicates that SOC is more easily produced on V_4/TiO_2 than V_4/ZrO_2. Similarly, compared Fig. 2a with b, it can also be found that SOC appears under the $(NO + O_2)$/He atmosphere at 100 °C, while it forms under the O_2/He atmosphere until the reaction temperature reaches 200 °C on V_4/ZrO_2 samples. It can be concluded that SOC is more easily produced under the $(NO + O_2)$/He atmosphere than under the O_2/He atmosphere. The results indicate that the presence of NO in reaction gas stream can promote the production of SOC species. Combined with the results of the catalytic activities in Table 1, it can be concluded that the formation of SOC species not only lower the peak temperatures of soot oxidation (T_m), but also it increases the selectivity to CO_2 formation (S_{CO_2}). In a word, the results of in-situ UV-Raman and the catalytic activity measurements demonstrate the formation of SOC is a fundamental process taking place in the catalytic soot oxidation over V_4/ZrO_2 and V_4/TiO_2 samples.

On the other hand, some reports have demonstrated that NO_2 is much more reactive towards soot oxidation than NO or O_2. Oi-Uchisawa et al. [6, 7] reported that a platinum catalyst could oxidize NO to NO_2, which subsequently oxidize soot to CO and CO_2. Thus, NO_2 is used as an intermediate to facilitate an indirect contact between the platinum catalyst and soot. This mechanism subtly changed solid (soot)–solid (catalyst) contact into solid (soot)–gas (NO_2)–solid (catalyst) contact. Thus, the platinum catalyst system obtained the best results so far reported for soot oxidation under loose contact conditions. The high oxidation rate of soot is due to the strong oxidizing ability of NO_2. A similar mechanism is found for soot oxidation over the V_4/TiO_2 catalyst in this study. As shown in Fig. 3, the direct evidence of NO_2 formation over the V_4/TiO_2 sample is first found by means of UV-Raman spectroscopic measurement. Due to the strong oxidation capacity of NO_2, the soot oxidation can be remarkably accelerated by NO_2. Therefore, V_4/TiO_2 catalyst has higher activity than V_4/ZrO_2 catalyst. This conclusion is verified by the results of the catalytic activities in Table 1. If NO is not contained in the reactant gases, the discrepancy of T_m is only 5 °C and $S^m_{CO_2}$ is almost same for soot oxidation over V_4/ZrO_2 or V_4/TiO_2 catalysts. Whereas, when NO is present in the reactant gas stream, compared to soot oxidation over V_4/ZrO_2 catalyst, T_m decreases by 44 °C and $S^m_{CO_2}$ increases by 2% point for that over V_4/TiO_2 catalyst.

The combination of fundamental molecular structural information and in-situ UV-Raman spectra has resulted in a molecular-level understanding of structure–activity relationships for soot oxidation reaction. Taking into account the above experimental results and discussion, two different reaction mechanisms can be proposed for soot oxidation over V_m/ZrO_2 or V_m/TiO_2 samples.

Mechanism 1:

$$O_2(g) \rightarrow 2O_{ads/M_xO_y} \quad (1)$$

$$O_{ads/M_xO_y} \rightarrow O_{ads/C} \quad (2)$$

$$C_f + O_{ads/C} \rightarrow C_f(O) \quad (3)$$

$$C_f(O) + O_{ads/C} \rightarrow SOC \quad (4)$$

$$SOC + O_{ads/c} \rightarrow C_f(O) + CO_2(g) \quad (5)$$

$$SOC + O_{ads/C} \rightarrow C_f(O) + CO(g) \quad (6)$$

where, M_xO_y refers to V_4/ZrO_2 or V_4/TiO_2 catalysts, and C_f refers to reactive free carbon, and $C_f(O)$ refers to the unreactive surface oxygen complexes, and SOC stands for the reactive surface oxygen complexes. According to our previous results [1, 17–19], the catalytic active sites of supported vanadia catalysts for soot oxidation reaction are mainly polymeric vanadyl V–O–V species, while crystalline bulk V_2O_5 and isolated vanadium oxide are supposed

Table 1 The peak temperature (T_m) and the selectivity to CO_2 formation at T_m temperature $S^m_{CO_2}$ for soot oxidation over V_4/ZrO_2 or V_4/TiO_2 catalysts at different reactant gas compositions

Catalysts	V_4/ZrO_2	V_4/ZrO_2	V_4/TiO_2	V_4/TiO_2
Reactant gas compositions	5% O_2 + 0.2% NO + He	10% O_2 + He	5% O_2 + 0.2% NO + He	10% O_2 + He
T_m (°C)	433	435	389	430
$S^m_{CO_2}$ (%)	89	87	90	87

to be less active than polymeric surface vanadyl species. V_4/ZrO_2 or V_4/TiO_2 catalysts have high concentration of polymeric vanadyl species. Thus, the active sites of M_xO_y should be V–O–V species supported on ZrO_2 or TiO_2 supports. Moreover, the difference between O_2 and O_{ads} should be explicitly noticed. O_2 denotes a much more free state of oxygen, being mobile by surface migration on the edges or basal plane of the carbonaceous material, and O_{ads} stands for the adsorption oxygen on the surface of catalyst. In the above notation, $C_f(O)$ and SOC refer to surface oxygen complexes in which the chemical interaction between the carbon and oxygen atom is so strong that the oxygen atom can be considered to be chemically bonded. In the literature [13, 16], these surface oxygen complexes may be composed of carbonyl and ether groups as lactone, quinine, and acid anhydride functional groups. However, SOC are typically composed of carboxyl in this work. This mechanism is consistent with the reference [16].

Gaseous oxygen is adsorbed dissociatively on the catalyst surface (reaction 1) and then the oxygen atoms adsorbed on soot ($O_{ads/C}$) are formed by the transferring of O_{ads} to the surface of soot (reaction 2). The resulting species attack the reactive free carbon to give the unreactive surface oxygen complex intermediate $C_f(O)$ (reaction 3). They react with $O_{ads/C}$ to produce reactive surface oxygen complex intermediate SOC (reaction 4). These complexes exist as carboxyl groups (COO^-). $O_{ads/C}$ is added to such complexes through reaction, and upon desorption of a CO and a CO_2 gaseous product molecules an adjacent carbon atom forms a new complex (reactions 5 and 6). Surface oxygen complexes increase the rates of catalytic oxidation of Printex U. CO_2/CO ratios also increase in the presence of surface oxygen complexes.

For soot oxidation over V_4/ZrO_2 catalyst, only SOC intermediate species are detected and the reaction mainly follows the mechanism 1. Thus, the whole reaction mechanism can be described in the Fig. 4a. For soot oxidation over V_4/TiO_2 catalyst, NO_2 is also detected besides SOC. Therefore, the following reaction process must be considered besides the mechanism 1 shown above.

Mechanism 2:

$$O_2 + 2NO \rightarrow 2NO_2 \quad (7)$$

$$2NO_2 + C \rightarrow 2NO + CO_2 \quad (8)$$

$$NO_2 + C \rightarrow NO + CO \quad (9)$$

Thus, both the formation of SOC and the production of NO_2 play important roles in soot oxidation over V_4/TiO_2 catalyst. In other words, two reaction pathways to oxidize soot take place simultaneously over V_4/TiO_2 catalyst. The whole reaction process can be described in the Fig. 4b.

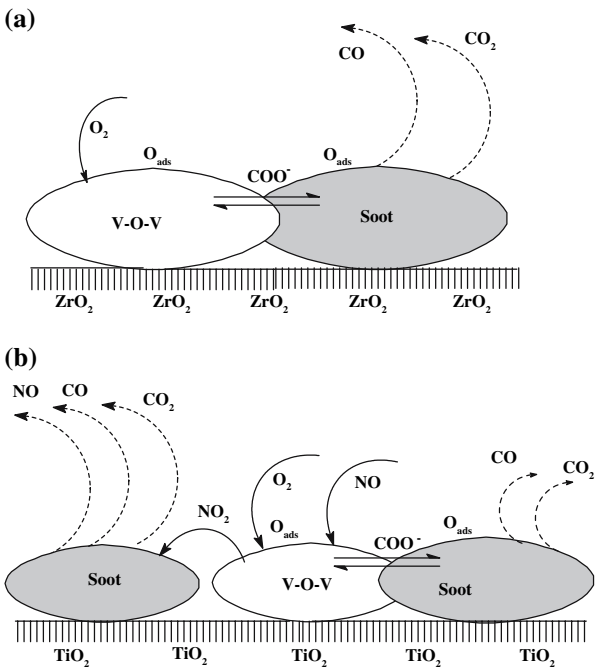

Fig. 4 The schemes of the reaction mechanisms for soot oxidation over V_4/ZrO_2 or V_4/TiO_2 catalysts: (**a**) V_4/ZrO_2 and (**b**) V_4/TiO_2

4 Conclusions

The formation of carboxyl group species in the catalytic oxidation of soot over V_4/ZrO_2 and V_4/TiO_2 catalysts was observed by in-situ UV-Raman spectroscopy. The presence of NO in the reaction gas stream can promote the formation of SOC species. Based on the in-situ UV-Raman experimental results, two different reaction mechanisms to oxidize soot over V_4/ZrO_2 or V_4/TiO_2 samples are proposed. For soot oxidation over V_4/ZrO_2 catalyst, only SOC intermediate species are detected and the reaction mainly follows the mechanism of the formation of SOC. For soot oxidation over V_4/TiO_2 catalyst, NO_2 is also detected besides SOC. The reaction simultaneously follows both the mechanism of the formation of SOC and the mechanism of the indirect catalysis of NO_2.

Acknowledgments This work was supported by the National Natural Science Foundation of China (Nos. 20473053 and 20525021), the Beijing Natural Science Foundation (No. 2062020), the 863 Program of China (No. 2006AA06Z346), and the Scientific Research Key Foundation for the Returned Overseas Chinese Scholars of State Education Ministry.

References

1. Liu J, Zhao Z, Xu C, Duan A, Zhu L, Wang X (2005) Appl Catal B 61:36
2. Zhao Z, Liu J, Xu C, Duan A, Kobayashi T, Wachs IE (2006) Top Catal 38:309

3. Setiabudi A, Allaart NK, Makkee M, Moulijn JA (2005) Appl Catal B 60:233
4. Mul G, Neeft JPA, Kapteijn F, Moulijn JA (1998) Carbon 36: 1269
5. Minogue N, Riordan E, Sodeau JR (2003) J Phys Chem A 107: 4436
6. Oi-Uchisawa J, Obuchi A, Wang SD, Nanba T, Ohi A (2003) Appl Catal B 43:117
7. Oi-Uchisawa J, Wang SD, Nanba T, Ohi A, Obuchi A (2003) Appl Catal B 44:207
8. Sadezky A, Muckenhuber H, Grothe H, Niessner R, Poschl U (2005) Carbon 43:1731
9. Alvarez-Puebla RA, Garrido JJ, Aroca RF (2004) Anal Chem 76:7118
10. Amariei D, Coutheoux L, Rossigno S, Kappenstein C (2007) Chem Eng Process 46:165
11. Minogue N, Riordan E, Sodeau JR (2003) J Phys Chem A 107:4436
12. Kim UJ, Furtado CA, Liu X, Chen G, Eklund PC (2005) J Am Chem Soc 127:15437
13. Mul G, Kapteijn F, Moulijn JA (1997) Appl Catal B 12:33
14. Zhang J, Li M, Feng Z, Chen J, Li C (2006) J Phys Chem B 110:927
15. Li C (2003) J Catal 216:203
16. Stanmore BR, Brilhac JF, Gilot P (2001) Carbon 39:2247
17. Liu J, Zhao Z, Xu C, Duan A, Zhu L, Wang X (2006) Catal Today 118:315
18. Liu J, Zhao Z, Xu C (2005) Acta Phys-Chim Sin 21:156
19. Liu J, Zhao Z, Xu C (2005) Chem J Chinese U 26:1290